A preliminary process mineralogical study for revalorisation of the Storgangen tailings, SW Norway

Bendik Standal Frantzen[a], Bjørn Eske Sørensen[a] and Kurt Aasly[a]

[a]Department of Geosciences, Norwegian University of Science and Technology, S.P. Andersens veg 15a, 7031 Trondheim, Norway

*Corresponding author: bendik.frantzen@ntnu.no

Keywords

Tailings, revalorisation, Storgangen, process mineralogy, ilmenite, magnetite, sulphides.

1. Introduction

An estimated 8.85 to 14.4 billion tonnes of tailings are produced each year (Oberle, Brereton, & Mihaylova, 2020). The total volume of mine tailings that exists worldwide is 45.5 billion m^3 as of 2020, accounted for only by the 1743 tailings storage facilities with known data (United Nations Environment Programme, International Council on Mining and Metals, Principles for Responsible Investment, 2020). The total number of tailings storage facilities is estimated at around 8500, making the actual volume of mine tailings likely far higher (United Nations Environment Programme, International Council on Mining and Metals, Principles for Responsible Investment, 2020).

The variety of elements utilised has increased dramatically in the recent century. In antiquity, only seven metals were known and used: Au, Ag, Cu, Fe, Hg, Pb, and Sn (Habashi, 2013). Of the 83 stable elements on the periodic table, an average of 62 are used in modern smartphones (Bookhagen, et al., 2020; Magrini, Verga, Bassani, Pirri, & Azim, 2025). In the first cars produced, only 5 to 10 elements were used, compared to the 76 elements used to produce modern electric vehicles (Bhuwalka, et al., 2021).

Due to the rising global demand for raw materials, high supply risks and import dependence on global superpowers in a geopolitical climate where export limits can be weaponised, the EU set clear domestic targets for critical raw material production with the European Critical Raw Materials Act (European Commission, 2024). The targets state that by 2030, 10% of the EU's annual consumption is to be met by domestic extraction, at least 40% must be processed in the EU, and at least 25% must come from recycling. In the fourth and latest

edition, the critical raw materials list of the European Commission contains 30 materials, including titanium metal, cobalt and vanadium (European Commission, 2020).

The decline in worldwide ore grades and the growing need for critical raw materials have shifted the view of mine tailings from mine waste to a potential secondary resource (Calvo, Mudd, Valero, & Valero, 2016; Blengini, Mancini, Mathieux, Nyberg, & Viegas, 2019). Historic mine tailings may contain critical minerals and elements that were not economically viable when they were operational.

The historic Storgangen mine produced ilmenite for the pigment industry and magnetite for iron production (Carstens, 2002). After production ended, the Storgangen mine had deposited an estimated 6 million tonnes of mine tailings into the Sandbekk mine tailings storage facility (Nilsen, 2015). With improved processing methods and higher recovery since the 1960s, the Storgangen mine tailings could contain viable secondary Fe-Ti-V and sulphide resources. This paper presents a preliminary process mineralogical study for revalorising Storgangen mine tailings for Fe-Ti-V and Ni-Cu-Co.

2. Background

2.1 Regional geology and the Storgangen ilmenonorite deposit

The Storgangen deposit is hosted within the Åna-Sira Anorthosite Massif of the Rogaland Anorthosite Province. The Rogaland Anorthosite Province (RAP) is a roughly 1000 km^2 region of Proterozoic-type anorthosite on the south-western coast of Norway (Duchesne & Bingen, 2001; Ashwal & Bybee, 2017). It was formed at the margins of Sveconorwegian granulite facies migmatitic gneisses of the Fennoscandian Shield during ~100 Myr of the Meso- to Neoproterozoic (Schärer, Wilmart, & Duchesne, 1996; Slagstad, Roberts, Marker, Røhr, & Schiellerup, 2013; Bybee, et al., 2014; Slagstad, et al., 2022). The Rogaland Anorthosite Province consists of three main massifs, listed from the north-west to the south-east: the Egersund-Ogna massif, the Håland-Helleren massif, the Åna-Sira massif, and two smaller anorthosite-leuconorite bodies, the Garsaknatt massif to the east, and the Hidra massif to the south (Marker, Bolle, Robins, Meyer, & Schiellerup, 2004). Large areas of the eastern part of the Rogaland Anorthosite Province are overlain by the Bjerkreim-Sokndal layered intrusion, an up to 7000 metre-thick layered intrusion of anorthosite-kindred rocks (Wilson, Robins, Nielsen, Duchesne, & Vander Auwera, 1996).

The Rogaland Anorthosite Province hosts many Fe-Ti-P deposits of varying scale and importance. Three types of Fe-Ti-P deposits are identified by Duchesne (1999) based on their main ore mineral assemblage: Type 1: hemo-ilmenite; Type 2: hemo-ilmenite and titanomagnetite; Type 3: titanomagnetite, ilmenite and apatite. Two Type 2 deposits from the Åna-Sira massif are of international significance: the actively mined Tellnes deposit and the historic Storgangen deposit. The two deposits are about 4.5 km apart. The Storgangen deposit was mined from 1916 to 1965 (Titania A/S., 1992). In the year 1954, the Tellnes deposit was discovered after a systematic aerial magnetic survey for new deposits to replace the Storgangen operation (Titania A/S., 1992). Mining of the Tellnes deposit began in 1960, and during 1960 to 1965, both deposits were mined simultaneously.

The Storgangen deposit is a 4 km long and up to 60 metre thick, semicircular, modally layered norite dyke within the Åna-Sira massif anorthosites (Schiellerup, 1996). The orebody has several offshoots which can be followed up to 2 km away from the main dyke. The modal layering ranges from anorthositic and leuconoritic to noritic and melanoritic downwards in the deposit, with the composition of the cumulates ranging from 20 to 50 Wt.% hemo-ilmenite, 5 to 20 Wt.% magnetite, 20 to 40 Wt.% orthopyroxene, and 10 to 30 Wt.% plagioclase, and with typical accessory minerals biotite, green spinel, apatite, pyrite, chalcopyrite, pyrrhotite, pentlandite and zircon (Schiellerup, 1996). A recent systematic study of the stratigraphy of the Storgangen deposit was carried out by Mansur et al. (2025). Mansur et al. describe the ore as massive, medium-grained ilmenite- and magnetite-rich norite at the base of the deposit, with a gradual thinning of the layers upwards in the stratigraphy. Mansur et al. propose that the Storgangen deposit represents a staging chamber within the Rogaland Anorthosite Province, and that the deposit formed at 40% crystallisation of the parental magma, with the gravitational accumulation of Fe-Ti oxides at the bottom of the staging chamber.

2.2 Deportment of Fe-Ti-V and Ni-Cu-Co in the Storgangen deposit

The mineralogy of the Storgangen deposit comprises predominantly hemo-ilmenite and magnetite as primary ore minerals, and plagioclase and orthopyroxene as the primary gangue minerals (Krause & Pape, 1975; Schiellerup, 1996; Mansur, et al., 2025). The mineralogy of the Storgangen deposit is comparable to that of the Tellnes deposit, but the Tellnes deposit is more homogeneous and has additions of olivine and clinopyroxene, which are lacking in the Storgangen deposit (Kullerud, 2003; Kullerud, 2007; Mansur, et al., 2025). The main host of Ti in the Storgangen deposit is hemo-ilmenite. Other contributions are biotite and rutile, resulting from the rutilisation of ilmenite. Rutile appears within the hemo-ilmenite of the Storgangen ore as small and distinct

grains (Krause & Pape, 1975). The biotite content of the ore is typically less than 1 vol.% and the theoretical degree of Ti enrichment in micas ranges from 2.59 to 9.41 Wt.% TiO_2 (Krause & Pape, 1975; Namur, et al., 2009). The main contributors to the total Fe content of the deposit are ilmenite, orthopyroxene, magnetite, and minor biotite. The main hosts of V in the deposit are hemo-ilmenite and magnetite, with 0.27 and 0.96 Wt.% V_2O_3, respectively (Duchesne J.-C. , 1999).

The sulphides of the Storgangen deposit were described in Krause & Pape (1975) as mainly composed of complex particles spread evenly within the ore-hosted rocks, and as a tiny proportion as infills in fractures and veinlets. The primary sulphide minerals of Storgangen were pyrrhotite and chalcopyrite, but during cooling the pyrrhotite altered to pyrite and secondary magnetite, which is now the dominant assemblage of the complex sulphide particles in the ore (Krause & Pape, 1975). In the remaining pyrrhotite and chalcopyrite particles, pentlandite ($(Ni,Fe)_9S_8$) is present, typically presented with exsolution flames in the pyrrhotite. Krause & Pape describe the pentlandite to be mostly partially bravoitised, resulting in bravoite ($(Fe,Ni)S_2$) as well as the Co-Ni sulphide siegenite ($CoNi_2S_4$). In the pyrrhotite-free sulphide particles, millerite (NiS) is described as the primary nickel sulphide.

No detailed description with chemical assaying exists for the sulphides of the Storgangen deposit. A more recent detailed study of the Tellnes sulphide concentrate describes the Ni-Cu-Co-related sulphide mineralogy of the Tellnes deposit (Osen, 2024). Ni-Cu-Co elemental deportment in the Tellnes sulphide concentrate was Ni: 42.57 % in pentlandite, 32.42 % in millerite, 19.81 % in violarite, 3.71 % in siegenite, and 1.35 % in Co-pentlandite; Cu: 99.32 % in chalcopyrite, and 0.41 % in pyrite; Co: 63.41 % in siegenite, 28.49 % in Co-pentlandite, 4.49 % in violarite, 2.95 % in pentlandite and 0.55% in pyrite (Osen, 2024).

2.3 The Storgangen tailings deposit

The Storgangen mine operated from 1916 to 1965 under Titania A/S (Titania A/S., 1992). During the forty-nine-year period of production, an estimated 6 million tonnes of tailings were deposited on the moor just south of the Storgangen mine at Sandbekk (Nilsen, 2015). The tailings deposit consists of a main area of roughly 16 hectares and two smaller areas. The main area of the Storgangen tailings deposit lies in Kjerdal, a roughly 350 by 500 metre natural, bowl-shaped depression on the moor in the area's rolling hills. To the west, it tapers into a smaller area on Hauglandsmyr, situated in lower, boggy terrain that stretches westward to the Ålgårdselv river, which runs past Sandbekk from Ålgård in the north-east to Hauge i Dalane in the south-west. The smaller area above the Storgangen deposit consists of an approximately 100 metres wide, steep, talus-like slope of tailings, several

tens of metres tall, situated against the north rockface of the open-pit ravine of the Storgangen mine, and a narrow 100-200 metre continuation eastwards at the bottom of the ravine. This part of the Storgangen tailings deposit lies directly above parts of the Storgangen underground facilities.

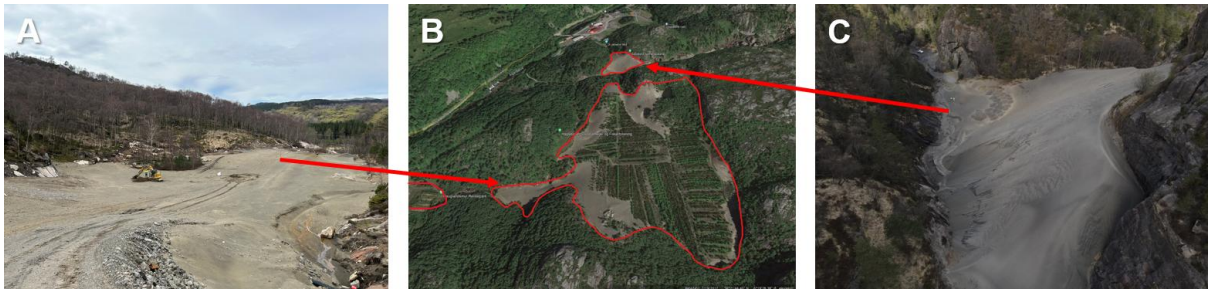

***Figure 1**: Sample location and overview of the Storgangen tailings deposit. **A)** Sample location for Storgangen tailings profiles 1 and 2 towards the Hauglandsmyr. **B)** Aerial view of the Storgangen tailings deposit in three parts outlined in red. **C)** Sample location for Storgangen tailings profiles 3 and 4. Situated on top of the main stope and the Engelske Stoller mine entrances to the historic Storgangen mine.*

2.4 Ore dressing, tailings deposition, and environmental impact of the Storgangen tailings deposit

Throughout the forty-nine-year life of the Storgangen mine, its processing methods changed. Comminution involved coarse crushing and milling the feed to a particle size below 1.5 mm. From the start of production until after the end of the Second World War, mineral separation was done by an initial shaking table step, followed by magnetic separation on specific shaking table fractions (Apeland, 1956). In the early 1950s, Titania A/S added a flotation step to the fines. For the first five years of production, from 1916 to 1920, the magnetite was deposited with the tailings because, due to its high titanium content, it was deemed unsellable (Carstens, 2002). From 1920, Titania A/S stored the magnetite, and from 1927 onwards the company could sell it. Sulphides were deposited together with the tailings (Nilsen, 2015).

No detailed description exists of how much tailings were deposited, where or when, at the Storgangen tailings deposit at Sandbekk, but a general overview is available (Carstens, 2002). The deposition of tailings at Sandbekk began at the Hauglandsmyr area towards the Ålgårdselv river. The Hauglandsmyr area was at capacity in the middle of the 1930s, and deposition commenced at the Kjerdal area, where the majority of the tailings were deposited. At this point, the coarse tailings were dewatered and deposited from the processing plant at Sandbekk onto the moor by a cable cart system. The untreated fine tailings were deposited directly into

the Ålgårdselv river. The tailings deposited in the ravine of the Storgangen mine are thought to represent the final stage of tailings deposition at Sandbekk.

Fine tailings deposited in the Ålgårdselv river are carried and merged into the greater Sokndalselv river, which flows through Hauge i Dalane and has its outlet into the sea at Sogndalsstranda roughly 6.5 km downstream from Sandbekk. After the operation at Sandbekk ended, the deposition ceased in 1965, and initial dredging of the harbour basin at Sogndalsstranda was carried out (Carstens, 2002). In 1967, the Sokndalselv river was lowered, resulting in greater sludge deposition in the harbour basin. Another round of dredging occurred in 1978, with costs split between the public and Titania A/S.

In October 1963, heavy downpours caused a landslide from the Hauglandsmyr part of the tailings deposit into the Ålgårdselv river, with an estimated 11 800 cubic metres of tailings (Carstens, 2002). The landslide led to work on stabilising the tailings deposit. Constructed wetlands and surface-water diversion systems were built. Natural vegetation on the Hauglandsmyr part stabilised that part of the tailings deposit. The main part of the tailings deposit at Kjerdal had issues with loss of tailings to windblown sand drift. Several revegetation campaigns at Kjerdal were unsuccessful until wind walls were used in combination with the successful planting of mountain pine from 1987 to 1992.

The main environmental impact of the Storgangen tailings deposit remains acid mine drainage, which results in elevated nickel contents. A water-treatment facility with artificial bogs was built on Hauglandsmyr, where it biologically leaches 90% of the Ni from the water (Nilsen, 2015). Despite the water-treatment facility's success, its capacity is limited, and much of the water from the Storgangen tailings deposit bypasses it.

3. Materials and methods

3.1 Materials

The materials of this study consist of four bulk samples of approximately 2 to 4 kg of wet and damp tailings material from the Storgangen tailings deposit. The samples were collected by excavating four profiles in the Storgangen tailings deposit and collecting wet or damp tailings material from below the water table using a plastic shovel (**Figure 2**). Profiles 1 and 2 reached the water table at depths of 0.8 and 1.3 metres, respectively, and material was collected in the 30 centimetres below the water table and placed in plastic sample buckets (**Figure 3**). At profiles 3 and 4, the water table could not be reached, and the materials were sampled at depths of 30 centimetres below 2.35 and 2.2 metres, respectively.



***Figure 2**: Images of the sampling campaign at the Sandbekk tailings storage facility from the Storgangen mine. **A**: Excavation of Profile 4. **B**: Image of Profile 2 with water leaking out of the bottom part. **C**: Overview of the excavation of Profile 4, with parts of the layered Storgangen intrusion and its wall anorthosite rock in the background.*

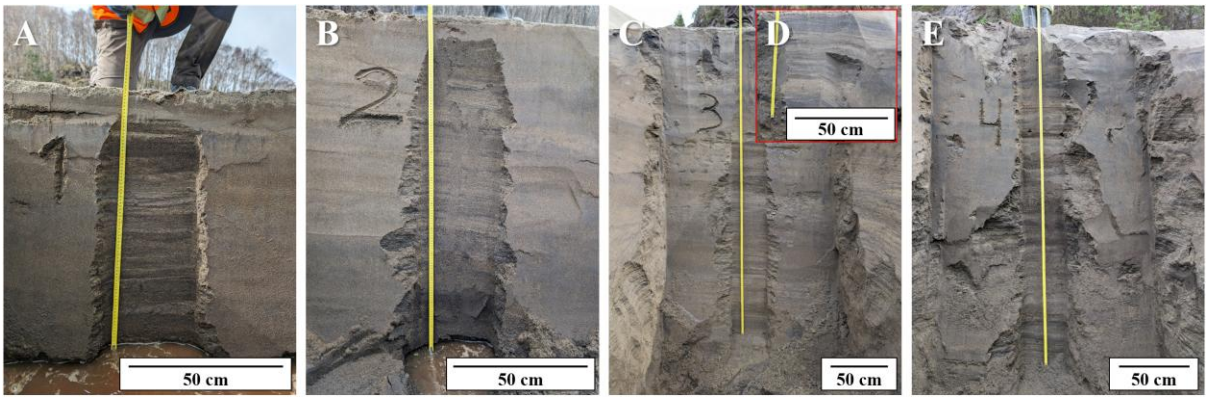

***Figure 3:** Tailings profiles 1 to 4, **1**: 601, **2**: 603, **3**: 605, **4**: 607. **A** and **B:** Tailings profiles 1 and 2 reached the water table at depths of 0.8 and 1.3 metres, respectively. **C** and **E**: Tailings profiles 3 and 4 did not reach the water table. The profiles were 2.35 and 2.20 metres deep. **D**: Close-up of dark (oxide) and light (silicate) layering within Profile 3. Section situated behind outcrop D in C.*

***Table 1**: Overview of the samples in the study and the respective analytical methods utilised. *Analysed externally at ALS Global in Loughrea, Ireland. Abbreviations: XRF – X-Ray fluorescence, OM – Optical microscopy, ICP-MS – Inductively coupled plasma spectrometry, SEM-AM – Scanning electron microscopy–based automated mineralogy, EPMA – Electron probe microanalysis.*

Sample name	Sieve weight (g)	Wt.%	Description	Instruments used
STO_T-601	1598	100	Bulk sample of Profile 1	XRF, XRF*, ICP-MS*
601_+425 µm	719	45.0	Sieved subsample of 601	XRF, OM, SEM-AM
601_+212-425 µm	504	31.5	Sieved subsample of 601	XRF, OM, SEM-AM, EPMA
601_+104-212 µm	273	17.1	Sieved subsample of 601	XRF, OM, SEM-AM
601_+53-104 µm	81	5.1	Sieved subsample of 601	XRF, OM, SEM-AM
601_-53 µm	21	1.3	Sieved subsample of 601	XRF, OM, SEM-AM
STO_T-603	767	100	Bulk sample of Profile 2	XRF, XRF*, ICP-MS*
603_+425 µm	227	29.6	Sieved subsamples of 603	XRF, OM, SEM-AM, EPMA
603_+212-425 µm	261	34.0	Sieved subsamples of 603	XRF, OM, SEM-AM, EPMA
603_+104-212 µm	180	23.5	Sieved subsamples of 603	XRF, OM, SEM-AM, EPMA
603_+53-104 µm	73	9.5	Sieved subsamples of 603	XRF, OM, SEM-AM, EPMA
603_-53 µm	26	3.4	Sieved subsamples of 603	XRF, OM, SEM-AM, EPMA
STO_T-605	927	100	Bulk sample of Profile 3	XRF, XRF*, ICP-MS*
605_+425 µm	247	26.6	Sieved subsamples of 605	XRF, OM, SEM-AM
605_+212-425 µm	311	33.5	Sieved subsamples of 605	XRF, OM, SEM-AM, EPMA
605_+104-212 µm	233	25.2	Sieved subsamples of 605	XRF, OM, SEM-AM
605_+53-104 µm	108	11.7	Sieved subsamples of 605	XRF, OM, SEM-AM
605_-53 µm	28	3.0	Sieved subsamples of 605	XRF, OM, SEM-AM
STO_T-607	1246	100	Bulk sample of Profile 4	XRF, XRF*, ICP-MS*
607_+425 µm	696	55.9	Sieved subsamples of 607	XRF, OM, SEM-AM
607_+212-425 µm	280	22.5	Sieved subsamples of 607	XRF, OM, SEM-AM, EPMA
607_+104-212 µm	171	13.7	Sieved subsamples of 607	XRF, OM, SEM-AM
607_+53-104 µm	77	6.1	Sieved subsamples of 607	XRF, OM, SEM-AM
607_-53 µm	22	1.8	Sieved subsamples of 607	XRF, OM, SEM-AM

3.2 Sample preparation

The wet and damp material of each sample was dried at NTNU on a Borel heating table at 60°C for 48 hours. The sample material was deagglomerated manually and bagged. The dried bulk subsamples 601 (2111 g), 603 (2723 g), 605 (1865 g) and 607 (1798 g) were split at NTNU into ten roughly 180-270 g subsamples based on the bulk total mass using a rotary splitter, and one subsample from each profile was kept for external analyses at ALS Global in Loughrea, Ireland.

3.3 Particle size analyses

Prior to shipping the sample material from Titania A/S to the Department of Geosciences of the Norwegian University of Science and Technology, hereby referred to as NTNU, minor subsamples from each tailings profile were collected by Titania AS by inserting small sampling tubes into the buckets from each profile and removing whole sections of the sample material for internal particle-size distribution and XRF analyses. The particle size distribution of the bulk sample material from each profile was analysed by laser diffraction analysis at Titania AS using a Malvern Mastersizer 3000. The dried bulk subsamples from 601, 603, 605, and 607 were sieved in the split batches at NTNU using a W.S. Tyler ROTAP RX-29 H&B vibrating sieve tower for 20 minutes to produce five size fractions (+425 µm, +212-425 µm, +104-212 µm, +53-104 µm, and -53 µm). The sieves were cleaned by hand and in an ultrasonic bath, and dried between sieving batches to prevent contamination and accumulation of stuck material in the apertures. Due to the time required per sieving batch, the sieving continued until the finest -53 µm fraction reached a total mass of more than 20 g, ensuring enough material for further analyses. For XRF analyses, a 20-30 g subsample of the bulk samples and of each fraction of all four profiles was produced using a riffle splitter. The fractions were split sequentially using a riffle splitter with an aperture of 0.5 cm to achieve the desired mass. From the finest -53 µm fraction of each profile, 2 g of material was split for polished thin sections using a riffle splitter with an aperture of 0.3 cm. The bulk and fraction subsamples were prepared for XRF by micronising using a Retsch RS 200 vibratory disc mill for 2 minutes at 1200 rpm in a tungsten chamber.

3.4 Elemental characterisation

To characterise the major and trace elemental composition of the bulk and fraction samples, both in-house and external analyses were carried out. Major- and trace-element chemistry was analysed by XRF at NTNU. For major-element analysis, 2.5 g of sample material was weighed into a crucible and annealed in a Nabertherm B180 annealing furnace at 1000°C for 1 hour. The annealed material was weighed to account for LOI/GOI. A 0.5 g subsample of the annealed material was added to a platinum crucible and mixed together with 5 g of the flux 66/34 lithium tetraborate/metaborate. 60 µL lithium iodide was added to the platinum crucible, and the material was fused to a glass disc after being melted with a Claisse TheOx Advanced fusion instrument at 1080°C for 20 minutes. The fused glass discs were analysed for major elemental composition using the PANalytical Zetium 4 kW X-ray spectrometer at NTNU with the WROXI software. For trace-element analysis, 9.6 g of sample material and 2.4 g Licowax were mixed with a glass bead in a Fluxana HD Elektronik mixing

instrument for 2 minutes. The mixed material was pressed into a pellet using a Preplab Herzog pellet presser with 200 kN of force. The pressed pellets were analysed for trace-element composition using the PANalytical Zetium 4 kW X-ray spectrometer with the Pro-Trace software.

To validate the in-house analyses, a split of the bulk sample material from each profile was shipped to ALS Global in Loughrea, Ireland. At ALS, the sample material was pulverised to 85% passing 75 µm, before being analysed for main element chemistry by fused disc XRF (ALS Code: ME-XRF21n) and trace element chemistry by four-acid digestion ICP-MS (ALS Code: ME-MS61L) (ALS, 2026).

3.5 Optical microscopy and automated mineralogy investigations

Vertically cut polished powdered sections were produced for each fraction of the four profiles at NTNU following the procedure in Røisi (2018), totalling twenty sections. The sections were produced using 2.0 g of sample material for the +104-212 µm, +212-425 µm, and +425 µm fractions. To avoid particle agglomeration and resulting issues with automated mineralogy analyses of the two finest fractions, -53 µm and +53-104 µm, 1.5 g of sample material was mixed with 1 g of graphite powder according to the ratios in Røisi and Aasly (2018).

Optical microscopy studies with reflected light and automated mineralogy analyses were carried out at the Norwegian Laboratory for Mineral and Materials Characterisation (MiMaC) at NTNU. The reflected-light optical microscopy studies were performed using a Nikon Eclipse LV100POL microscope, and photomicrographs were captured with a Nikon DS-FI2 camera. To determine modal mineralogy, mineral associations, mineral textures and mineral liberation, automated mineralogy analyses of each of the twenty polished sections were carried out using a ZEISS Sigma 300VP Field Emission SEM with two Bruker X-flash 6/60, 129 eV EDS detectors with the ZEISS Mineralogic and the Mining plugin. The analytical settings were 20 kV acceleration voltage, 8.5 mm working distance, and a 120 µm aperture. The EDS step size was 4 µm for the two finest fractions (-53 µm and +53-104 µm) and 8 µm for the three coarsest fractions (+104-212 µm, +212-425 µm, and +425 µm) of sample 603, and a step size of 5 µm for all fractions of samples 601, 605 and 607.

Post-processing of the automated mineralogy data involved snipping touching particles and optimising the mineral classification recipe to correctly represent mineral modes and textures. Automated mineralogy false colour mineral maps and corresponding BSE maps were produced for the scan of each sample. The automated mineralogy data were organised and presented in tables for bulk modal mineralogy, mineral associations,

elemental assays and mineral locking and liberation data. The liberation data produced are classified as area-grade liberation.

3.6 Electron probe microanalysis

The EPMA analyses on the polished powdered sections were run in the MiMaC laboratory at NTNU on a JEOL JXF-8530F PLUS Field Emission microprobe equipped with five wavelength-dispersive and one energy-dispersive spectrometers. The point analyses were run with a standard wavelength-dispersive setting with an accelerating voltage of 20 kV, a beam current of 20 nA, and a beam diameter of 1 μm.

The EPMA campaign aimed to identify variations in ilmenite and magnetite composition across fractions and between profiles. It consisted of 20 to 30 points in the mineral phases ilmenite and magnetite in all fractions of the 603 sample, and in the +212-425 μm fraction of the samples 601, 605, and 607. Where 30 points of ilmenite or magnetite were not possible, there are fewer points.

The analyses of the Storgangen ilmenite and magnetite were performed alongside a campaign on the Storgangen ore, resulting in an expanded element list. A total of 22 elements were analysed at each point: Si, P, Ta, Ti, Zr, Sn, W, Al, V, Cr, Fe, Ni, Mn, Co, Zn, Mg, Cu, Ca, Na, K, F, and Cl. The final paper will report the crystals, elemental order, dwell times, and peaks.

To obtain elemental Wt.% data, the ZAF matrix correction was applied to the raw X-ray data from the EPMA analyses. An interference correction was applied to Mg for interference from Zr, and to V for interference from Cr. The calibration standards used were the best available natural or synthetic standards for each relevant element. Iron was reported as Wt.% total FeO from the EPMA analyses. The FeO and Fe_2O_3 components for both the ilmenite and the magnetite analyses were recalculated and the totals adjusted for the extra oxygen.

4. Results

4.1 Particle size distribution

The particle size distribution analyses from Titania AS of the bulk samples of Profiles 1 to 4 of the Storgangen tailings fall almost fully within the whole sand size range, and with only 1.6 to 4 % of the cumulative volume being coarse silt (**Figure 4**). Samples 603 and 605 of Profiles 2 and 3 are the overall finest fractions and display similar PSD curves. Profile 1 – 601 is coarser, and Profile 4 – 607 is the coarsest of the four. Profiles 1 to 4 have

d50s of 356 µm, 276 µm, 284 µm, and 469 µm. As seen in **Figure 4**, there is little fine material, with Profiles 1 to 4 having d10s of 128 µm, 102 µm, 101 µm, and 115 µm, respectively. The two finest sieved fractions of the samples, -53 µm and +53-104 µm, constitute only 1.45 to 2.40 % and 5.00 to 8.98 % of the material (**Table 2**).

Reporting errors from Titania AS leave the data above d90 uncertain, and the curves (dotted) above d90 are extrapolated, given a maximum feed particle size for processing at Storgangen of 1.5 mm.

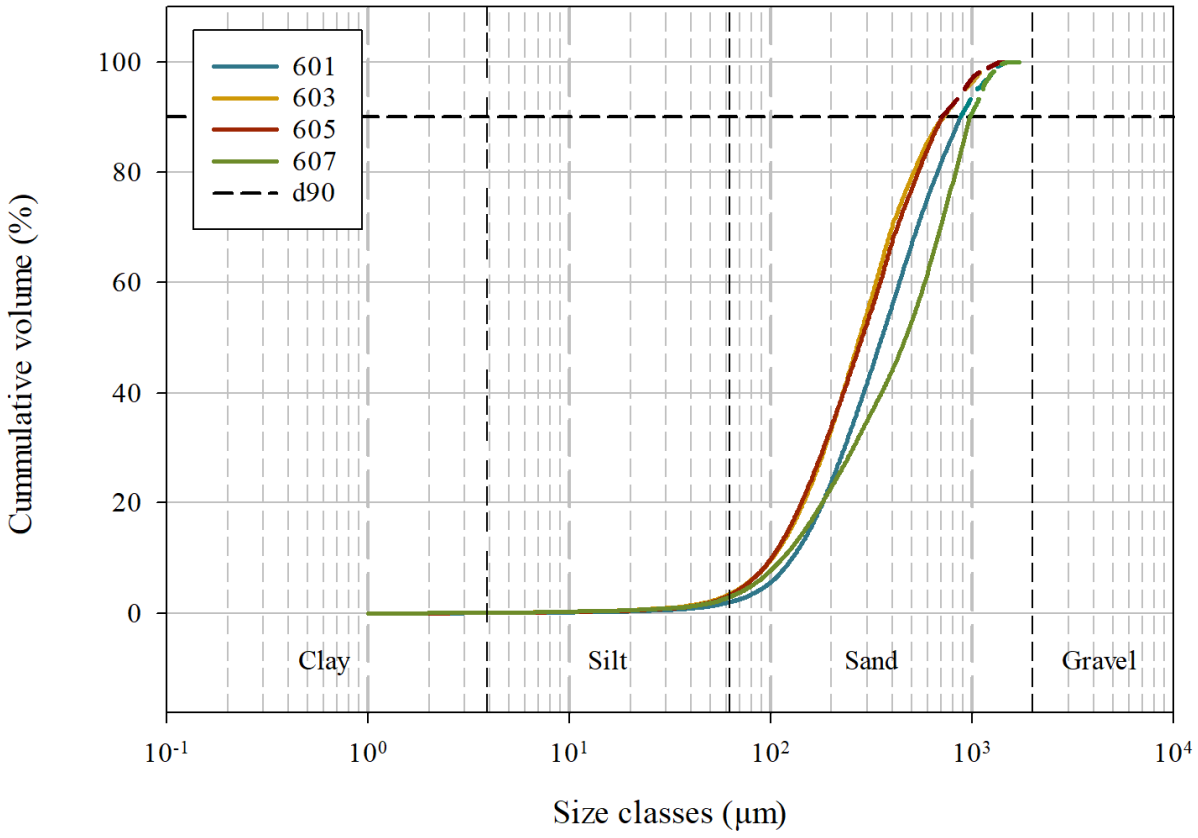

***Figure 4**: Particle size distribution of the tailings samples. D90 and above are extrapolated, given the 1.5 mm top size of the feed, and the line is stipulated. Particle classes following the Wentworth scale (Wentworth, 1922).*

***Table 2:** Cumulative volume of tailings by sieved fractions of Profiles 1 to 4 of the Storgangen tailings. C. Vol% = cumulative volume per cent, Avg. = average.*

Fraction Sample	-53 µm C. Vol%	+53-104 µm C. Vol%	+104-212 µm C. Vol%	+212-425 µm C. Vol%	+425 µm C. Vol%
Profile 1 - 601	1.45	5.00	19.78	32.65	41.12
Profile 2 - 603	2.4	8.48	25.42	36.46	27.24
Profile 3 - 605	2.22	8.98	25.26	33.66	29.88
Profile 4 - 607	2.07	6.65	15.77	21.75	53.76
Avg.	2.04	7.28	21.56	31.13	38.00

4.2 Elemental composition

The bulk chemistry analysis of Storgangen tailings profiles 1 – 4 shows that half of the bulk chemistry is SiO_2, with major components of Al_2O_3 and Fe_2O_3, and minor MgO, CaO, TiO_2 and Na_2O (**Table 3**). All four profiles are similar in elemental composition, but with some variations in TiO_2 and Fe_2O_3 contents. TiO_2 contents vary between 3.32 and 5.49 %, and Fe_2O_3 between 9.89 and 15.25 % in the NTNU analysis. Profile 2 has the highest Ti and Fe content, while Profile 4 has the lowest. Comparing the NTNU results with the external ALS analysis shows only subtle differences, with a maximum of ±0.2 % in the major elements.

Table 3: *Comparison of ALS and NTNU XRF analyses on the bulk sample material of Profiles 1 – 4. ALS XRF analysis code: ME-XRF21n (ALS, 2026).*

		Profile 1- 601		**Profile 2 - 603**		**Profile 3 - 605**		**Profile 4 - 607**	
Oxide / Element	**Unit**	**ALS**	**NTNU**	**ALS**	**NTNU**	**ALS**	**NTNU**	**ALS**	**NTNU**
SiO_2	**(%)**	48.20	48.09	46.40	46.26	47.90	48.15	49.90	49.90
P_2O_5	**(%)**	0.04	0.01	0.05	0.02	0.05	0.03	0.05	0.03
TiO_2	**(%)**	4.25	4.25	5.42	5.49	4.63	4.53	3.37	3.32
Al_2O_3	**(%)**	16.00	16.29	14.50	14.50	16.00	16.23	18.85	18.95
Fe_2O_3	**(%)**	13.42	12.86	15.61	15.25	13.62	12.89	10.42	9.89
Mn_3O_4	**(%)**	0.14	0.14	0.17	0.16	0.14	0.13	0.11	0.10
MgO	**(%)**	8.72	8.50	9.62	9.67	8.56	8.44	6.28	6.16
CaO	**(%)**	5.64	5.71	5.12	5.13	5.64	5.72	6.55	6.62
Na_2O	**(%)**	3.06	3.14	2.74	2.70	3.05	3.16	3.69	3.78
K_2O	**(%)**	0.48	0.50	0.43	0.43	0.50	0.51	0.60	0.62
Totals	**(%)**	99.95	99.49	100.06	99.61	100.09	99.79	99.82	99.37

The major and trace element analysis of bulk and sieved fraction samples shows a slight depletion of TiO_2, Fe_2O_3 and V in the two middle fractions, +104 µm and +212 µm, compared to the top size fraction and bulk samples (**Figure 5**). All three elements are enriched in the two finest fractions, -53 µm and +53 µm, with the highest contents in the finest fraction. With 4.53 - 5.19 % TiO_2 in the bulk samples to 10.04 – 13.30 % TiO_2 in the finest fraction across all profiles. Fe_2O_3 enriches from 9.89 – 15.25 % in the bulk samples to 24.01 – 33.76 % in the finest fraction. Vanadium content follows the TiO_2 and Fe_2O_3 trends, with an enrichment of V from 168 – 270 ppm in the bulk samples to 479 – 805 ppm in the finest fraction.

The sulphide elements Ni, Cu, and Co show little variation between the bulk sample contents and the four coarsest sieve fractions (+53 µm, +104 µm, +212 µm, and +425 µm), with values of 90 to 210 ppm of Ni, 80 to

210 ppm of Cu, and 60 to 125 ppm of Co (**Figure 6**). The samples of Profiles 1 and 4 show an enrichment of Ni and Co, and a significant enrichment of Cu in the finest fraction (-53 µm). Profile 2 shows a moderate enrichment of Ni, Cu, and Co, while Profile 3 displays the lowest increase from the bulk. In the finest fraction (-53 µm), Ni varies between 248 – 647 ppm, Cu between 904 – 4254 ppm, and Co between 127 -362 ppm.

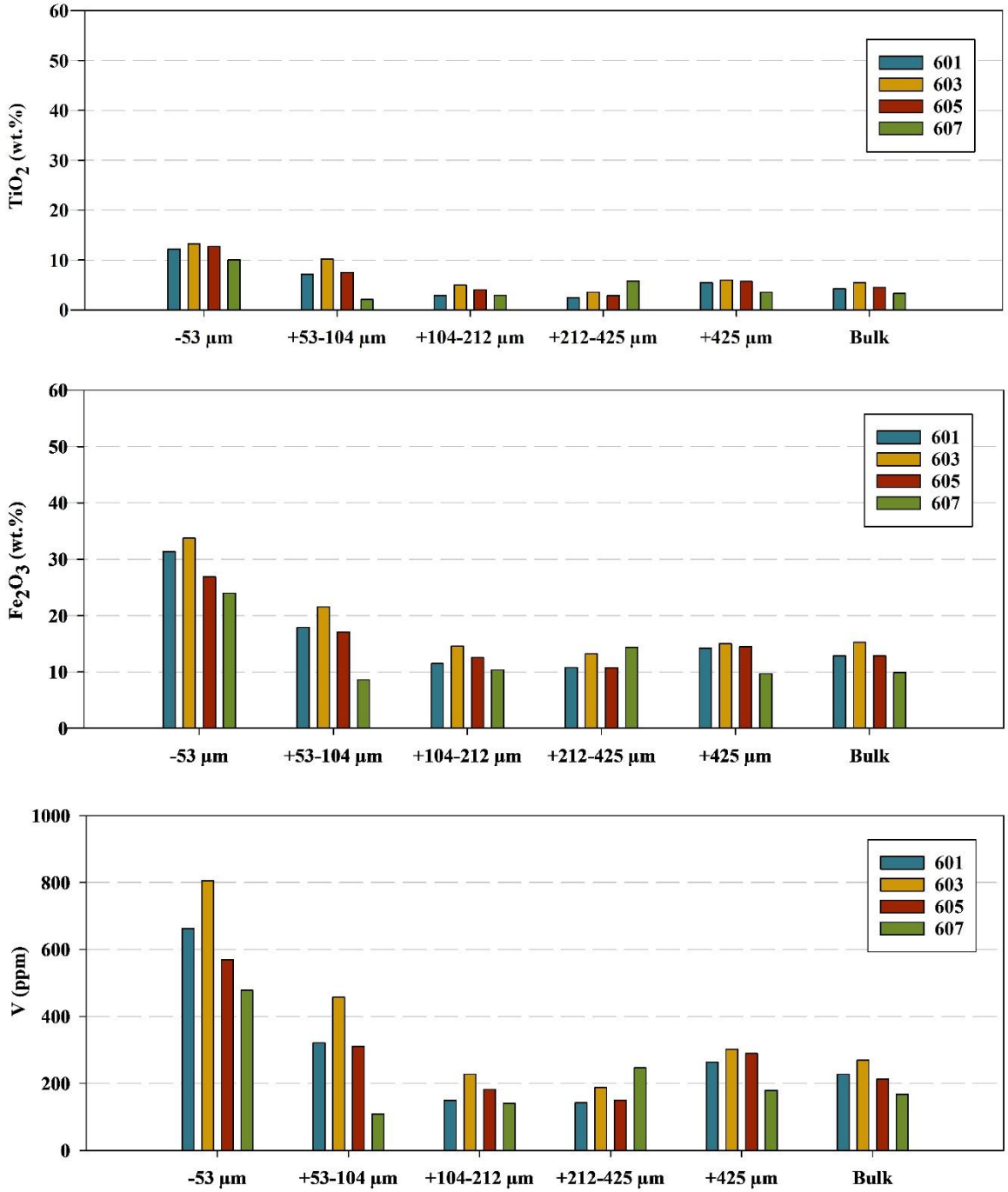

***Figure 5**: TiO_2 and Fe_2O_3 content by XRF main element, and V content by XRF trace element analysis in fractions and bulk samples. Based on results from analyses by NTNU.*

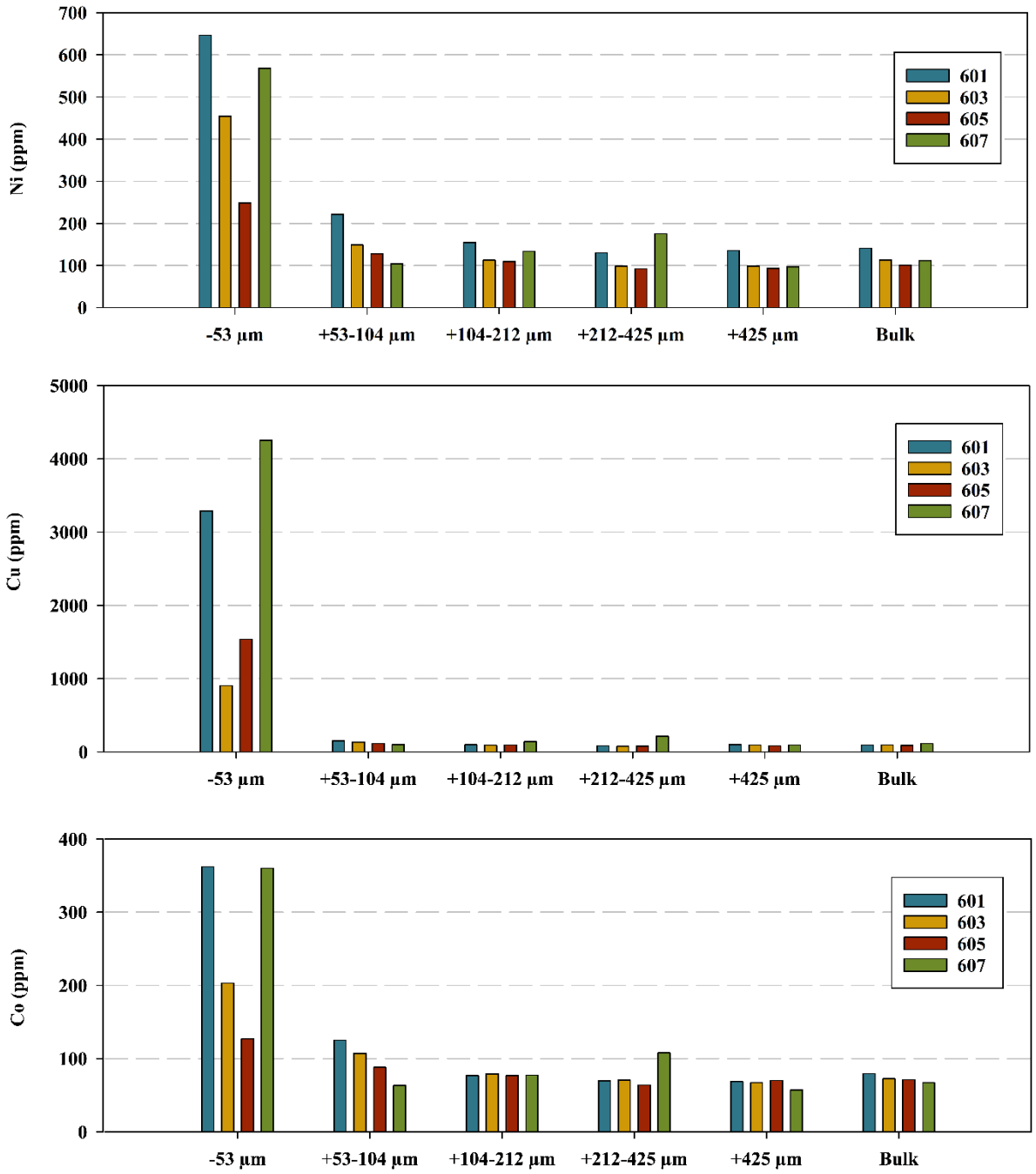

Figure 6: *Ni, Cu, and Co content by XRF trace element analysis in fractions and bulk samples. Based on results from trace element XRF analyses by NTNU.*

4.3 Modal mineralogy and ore mineral textures

The SEM scans with automated mineralogy yield full-section backscattered electron (BSE) and false colour scans of the polished powdered-fraction sections. For the false colour scans, a selection of colours was chosen to maximise visibility of ore, main gangue, and minor gangue minerals. For an example of false colour full section scans, see **Figure 7**. This extended abstract presents only the SEM-AM result for Profile 2 – 603; post-processing was not done for the remaining three profiles.

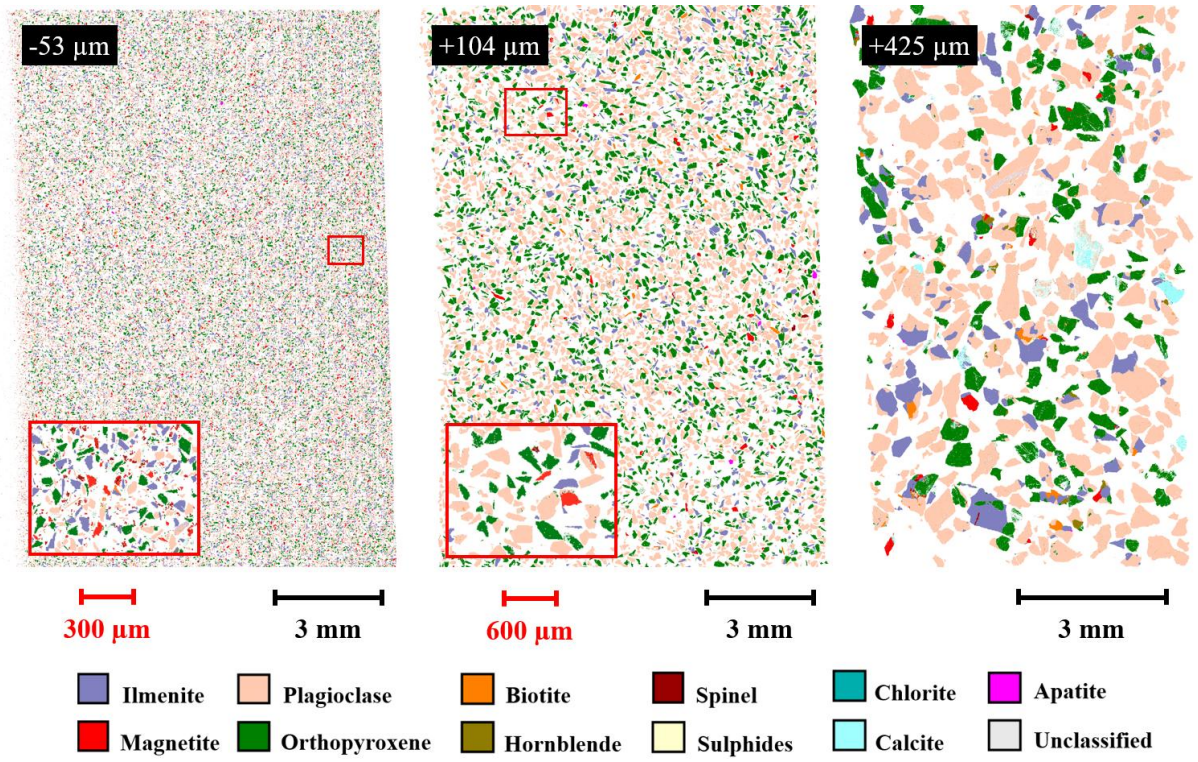

Figure 7: *AM false colour images from SEM scans of sections -53 µm, +104 µm, and +425 µm from Profile 2 – 603 from the Storgangen tailings. Red inserts show particle close-ups. The legend shows the main phases accounting for 1 Wt.% or more of the modal mineralogy, or of special interest, such as sulphides and apatite.*

The modal mineralogy results of Profile 2 – 603 show that the gangue minerals constitute the majority of the fractions +53 µm, +104 µm, +212 µm, and +425 µm by weight per cent, with the main gangue minerals being plagioclase, orthopyroxene, and minor chlorite, hornblende, and biotite (**Figure 8**). The top size (+425 µm) contains 19 Wt.% ilmenite and 2 Wt.% magnetite. The middle fractions (+104 µm and +212 µm) contain the lowest oxide content, with 0.7 Wt.% magnetite in both and 11 and 9 Wt.% ilmenite, respectively. In the +53 µm fraction, ilmenite enriches to 23 Wt.%, with magnetite at 1.7 Wt.%. In the finest fraction, -53 µm, ilmenite and magnetite constitute close to 45 Wt.% of the sample, with 28 Wt.% ilmenite and a large increase of 18 Wt.%

magnetite. Spinel content seems to follow the magnetite content across the fractions. Sulphides constitute only around 0.1 Wt% of the modal mineralogy of all fractions.

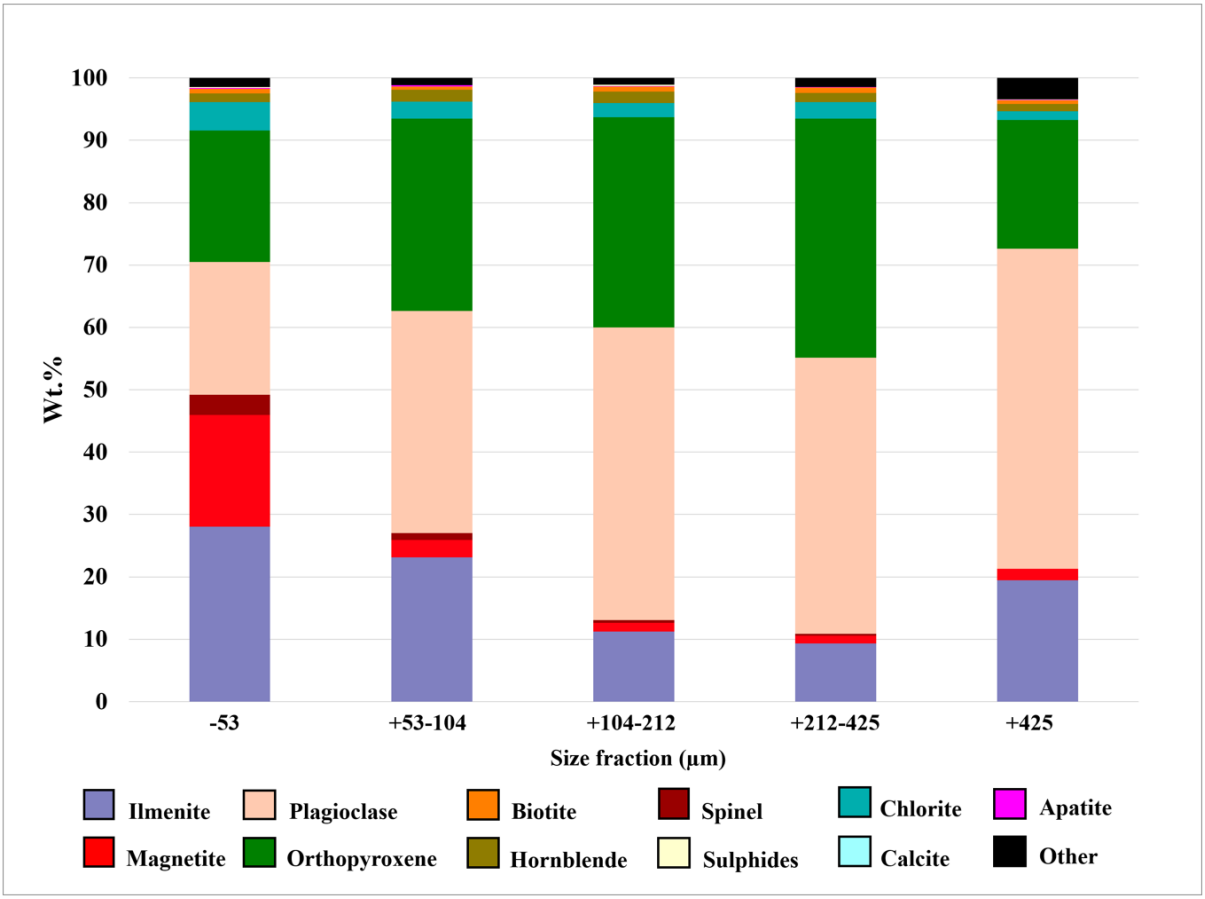

***Figure 8**: Modal mineralogy by weight per cent from SEM analyses of fractions from Profile 2 – 603 of the Storgangen tailings. Wt.% = weight per cent. The legend shows the main phases accounting for 1 Wt.% or more of the modal mineralogy, or phases of special interest, such as sulphides and apatite.*

In the polished sections, ilmenite mostly appears in composite particles with the main silicates or as liberated grains. Magnetite often accompanies ilmenite, if not as liberated grains, and tends to display more weathered surfaces (**Figure 9**). The ilmenite is textured with mostly homogeneous thin sub-micron hematite lamellae, and occasionally spinel needles. Magnetite is often observed associated with ilmenite, where a border of symplectic spinel and ilmenite separates the two phases. The ilmenite adjacent to the ilmenite and magnetite grain boundary, up to 100 microns, is free of visible hematite lamellae. The magnetite exhibits a range of fine (sub-micron) to coarser (up to 30 µm) spinel exsolution lamellae, and thin trellis-type ilmenite lamellae (1-5 µm) as described by van Gerve, Muchez, Nuorivaara & Namur (2026).

Sulphides are rarely observed within the polished sections. They either appear as “droplets” of sulphides within large composite particles in the coarsest fractions, or as small pyrite grains within weathered iron oxides in the finer fractions (**Figure 10**). Few to no liberated, discrete pyrite, pyrrhotite, chalcopyrite, pentlandite, or other sulphide phase grains are observed in the finer fractions.

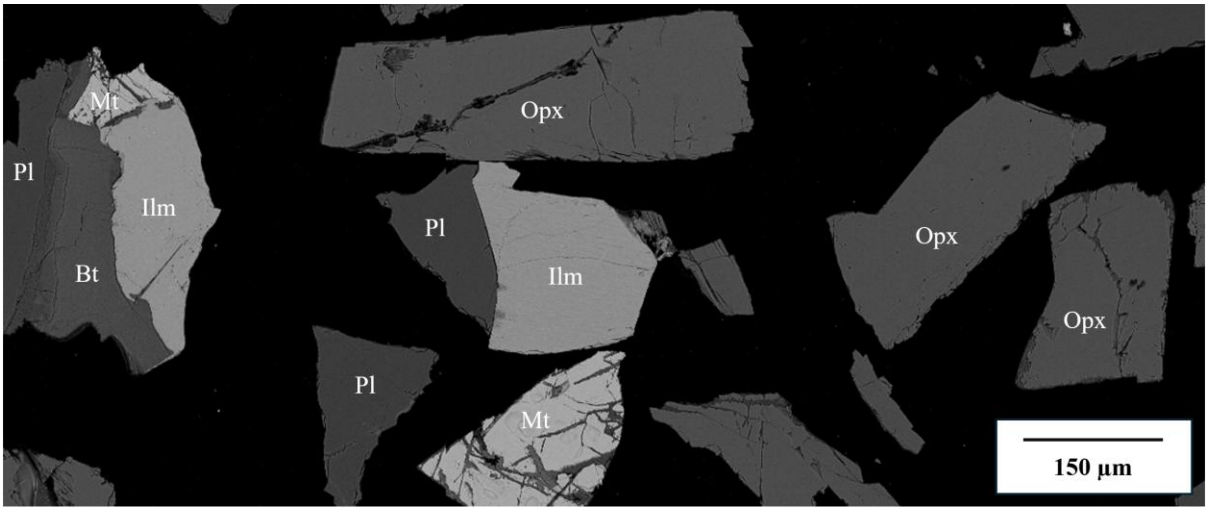

Figure 9: *Backscattered electron (BSE) image of particles from the +212 µm fraction of Profile 2 – 603 from the Storgangen tailings displaying typical composite particles of ilmenite, magnetite and the silicates. Fractured grains are typical of the tailings. The black background is the section epoxy. Ilm = ilmenite, Mt = magnetite, Pl = plagioclase, Opx = orthopyroxene, Bt = biotite. Mineral abbreviations according to IMA (Warr, 2021).*

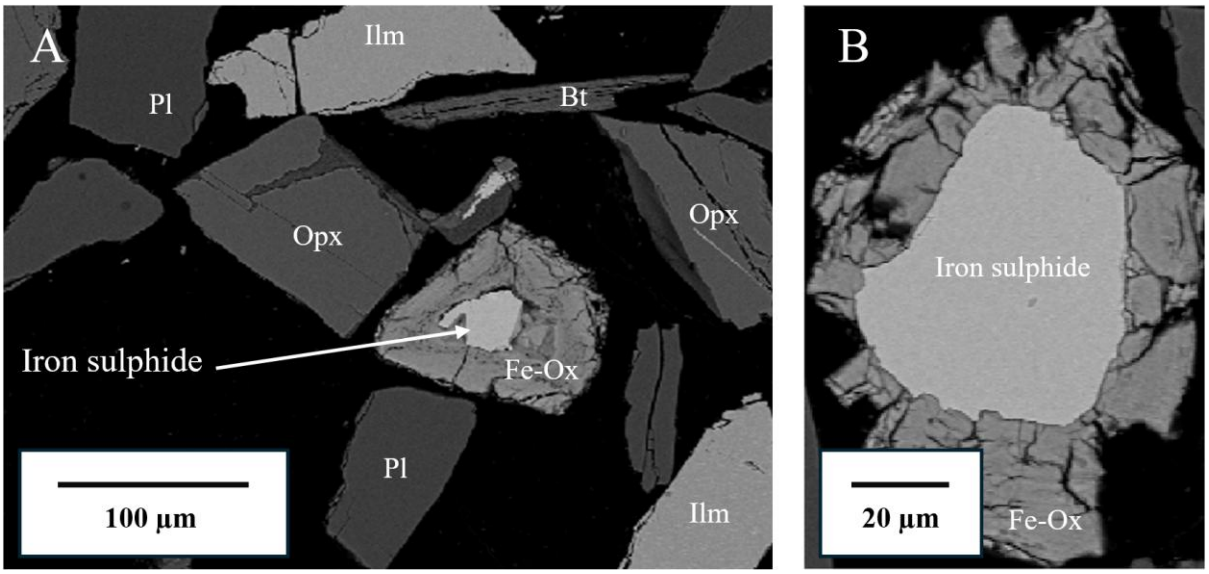

Figure 10: *Backscattered electron (BSE) image of particles from the +53 µm fraction of Profile 2 – 603 from the Storgangen tailings, displaying the typically observed sulphides in the tailings samples. Here, pyrite is displayed within weathered iron oxides. Fractured and weathered grains are typical of the tailings. The black background is the section epoxy. Ilm = ilmenite, Fe-Ox = iron oxide, Pl = plagioclase, Opx = orthopyroxene, Bt = biotite. Mineral abbreviations according to IMA (Warr, 2021).*

4.4 Mineral chemistry and internal variations

The EPMA results show little variation between the fractions of the Profile 2 – 603 sample, or across the +212 µm fraction of all four profiles. The average composition of the ilmenite is 45.86 Wt.% TiO_2, 36.78 Wt.% FeO, 11.99 Wt.% Fe_2O_3, 2.44 Wt.% MgO, 0.35 Wt.% MnO, and 0.22 Wt.% V_2O_5 with a total of 210 points (**Table 4**). The averages of fractions are close to the average of all points, except for the +212 µm fraction of the Profile 4 – 607 sample, which has slightly lower Fe_2O_3 and MgO contents. For the ilmenites, the Ti, Fe and Mg contents vary, with quite large standard deviations due to the varying solid solution of hematite and geikelite in the ilmenite. The MgO contents of all points typically fall closer to 0 Wt.% or closer to 3- 4 wt.%. The average composition of the ilmenite equals a solid solution of 78.35 % ilmenite, 11.56 % hematite, 9.32 % geikelite, and 0.76 % pyrophanite.

Table 4*: Electron probe microanalyses on ilmenite grains of the Storgangen tailings with components and average calculated formula. Sorted as min, max, average and standard deviation of all points, and by averages of each fraction and sample. N = number of points, Wt.% = weight per cent, Avg. = average, Stdev. = standard deviation. Ilm = ilmenite, Gk = geikelite, Pph = pyrophanite, Hem = hematite. Mineral abbreviations according to IMA (Warr, 2021).*

Mineral	**Ilmenite ($Ilm_{78.35}$,$Gk_{9.32}$,$Pph_{0.76}$,$Hem_{11.56}$)**												
Avg. Calculated formula	**($Fe^{2+}_{0.79}$,$Mg_{0.09}$,$Mn_{0.008}$)($Ti_{0.88}$,$Fe^{3+}_{0.23}$)O_3**												
N	**210**				**Sample**			**603**			**601**	**605**	**607**
		All points			**Fraction**	**+425**	**+212-425**	**+104-212**	**+53-104**	**-53**	**+212-425**	**+212-425**	**+212-425**
Wt.%	**Min**	**Max**	**Avg.**	**Stdev.**	**Avg. (N)**	**Avg. (31)**	**Avg. (31)**	**Avg. (19)**	**Avg. (19)**	**Avg. (20)**	**Avg. (30)**	**Avg. (30)**	**Avg. (30)**
SiO_2	0.14	0.67	0.21	0.07		0.16	0.17	0.16	0.17	0.17	0.21	0.36	0.22
P_2O_5	0.000	0.021	0.003	0.005		0.003	0.003	0.003	0.001	0.003	0.004	0.003	0.002
TiO_2	**39.81**	**49.76**	**45.86**	**1.53**		**45.73**	**46.24**	**46.26**	**45.68**	**45.95**	**45.54**	**45.44**	**46.18**
ZrO_2	0.000	0.059	0.009	0.012		0.006	0.008	0.011	0.008	0.012	0.006	0.008	0.011
WO_3	0.000	0.045	0.006	0.010		0.008	0.006	0.001	0.002	0.011	0.005	0.007	0.005
Al_2O_3	0.000	0.228	0.046	0.034		0.032	0.053	0.038	0.051	0.062	0.053	0.047	0.118
V_2O_5	**0.03**	**0.37**	**0.22**	**0.06**		**0.22**	**0.23**	**0.23**	**0.24**	**0.22**	**0.21**	**0.22**	**0.19**
Cr_2O_3	0.000	0.101	0.021	0.015		0.022	0.018	0.022	0.018	0.020	0.017	0.025	0.023
FeO	**31.95**	**42.34**	**36.78**	**1.83**		**36.47**	**37.16**	**36.85**	**36.34**	**36.36**	**36.29**	**36.45**	**38.02**
Fe_2O_3	**4.94**	**21.59**	**11.99**	**2.89**		**12.42**	**12.16**	**12.27**	**12.55**	**12.09**	**12.30**	**12.48**	**9.73**
NiO	0.000	0.148	0.023	0.033		0.014	0.023	0.030	0.019	0.023	0.034	0.016	0.030
MnO	**0.26**	**1.35**	**0.35**	**0.08**		**0.33**	**0.34**	**0.34**	**0.34**	**0.34**	**0.33**	**0.34**	**0.40**
ZnO	0.000	0.046	0.010	0.010		0.012	0.008	0.010	0.010	0.008	0.010	0.009	0.024
MgO	**0.03**	**3.70**	**2.44**	**0.95**		**2.53**	**2.40**	**2.58**	**2.58**	**2.70**	**2.57**	**2.52**	**1.89**
CaO	0.000	0.160	0.010	0.017		0.009	0.006	0.008	0.009	0.019	0.010	0.009	0.015
Na_2O	0.000	0.015	0.000	0.001		0.000	0.000	0.000	0.001	0.000	0.000	0.000	0.000
K_2O	0.000	0.021	0.002	0.003		0.002	0.002	0.002	0.003	0.002	0.002	0.003	0.002
F	0.000	0.011	0.002	0.003		0.002	0.002	0.003	0.001	0.003	0.001	0.002	0.001
Cl	0.000	0.041	0.003	0.005		0.001	0.003	0.004	0.004	0.008	0.002	0.002	0.004
Total	**96.04**	**99.58**	**97.99**	**0.69**		**97.98**	**98.83**	**98.84**	**98.04**	**98.00**	**97.60**	**97.95**	**96.86**

The magnetite is far purer than the ilmenite, with an average composition of 67.77 Wt.% Fe_2O_3, 30.49 Wt.% FeO, 0.89 Wt.% V_2O_5, 0.29 Wt.% Al_2O_3 and 0.23 Wt.% Cr_2O_3 with a total of 150 points (**Table 5**). Trace elements show little variation. The average V_2O_5 content of the magnetite is stable across all fractions analysed, ranging from 0.84 to 0.95 Wt.%.

***Table 5**: Electron probe microanalyses on magnetite grains of the Storgangen tailings with components and average calculated formula. Sorted as min, max, average and standard deviation of all points, and by averages of each fraction and sample. N = number of points, Wt.% = weight per cent, Avg. = average, Stdev. = standard deviation. Mt = magnetite, Usp = ulvöspinel. Mineral abbreviations according to IMA (Warr, 2021).*

Mineral	**Magnetite ($Mt_{99.6}$,$Usp_{0.4}$)**												
Avg. Calculated formula	**$(Fe^{2+}_{0.99})(Fe^{3+}_{1.97},Ti_{0.004},V_{0.023},Al_{0.013})O_4$**												
N	**150**				**Sample**			**603**			**601**	**605**	**607**
		All points			**Fraction**	**+425**	**+212-425**	**+104-212**	**+53-104**	**-53**	**+212-425**	**+212-425**	**+212-425**
Wt.%	**Min**	**Max**	**Avg.**	**Stdev.**	**Avg. (N)**	**Avg. (20)**	**Avg. (21)**	**Avg. (20)**	**Avg. (20)**	**Avg. (20)**	**Avg. (20)**	**Avg. (15)**	**Avg. (14)**
SiO_2	0.19	0.64	0.25	0.08		0.21	0.22	0.22	0.22	0.22	0.25	0.45	0.28
P_2O_5	0.000	0.022	0.003	0.005		0.002	0.004	0.006	0.003	0.002	0.003	0.003	0.002
TiO_2	**0.01**	**1.08**	**0.14**	**0.15**		**0.07**	**0.09**	**0.09**	**0.22**	**0.21**	**0.15**	**0.14**	**0.15**
ZrO_2	0.000	0.051	0.008	0.012		0.004	0.008	0.011	0.009	0.005	0.010	0.005	0.010
WO_3	0.000	0.064	0.009	0.014		0.010	0.009	0.009	0.003	0.008	0.008	0.015	0.011
Al_2O_3	0.01	0.99	0.29	0.13		0.24	0.32	0.28	0.29	0.30	0.29	0.30	0.25
V_2O_5	**0.14**	**1.09**	**0.89**	**0.16**		**0.95**	**0.87**	**0.91**	**0.89**	**0.94**	**0.80**	**0.89**	**0.84**
Cr_2O_3	0.00	0.44	0.23	0.07		0.24	0.19	0.23	0.25	0.24	0.21	0.24	0.23
FeO	**29.91**	**30.95**	**30.49**	**0.20**		**30.55**	**30.68**	**30.63**	**30.42**	**30.45**	**30.54**	**30.34**	**30.15**
Fe_2O_3	**66.48**	**68.80**	**67.77**	**0.43**		**67.91**	**68.19**	**68.09**	**67.61**	**67.68**	**67.89**	**67.45**	**67.02**
NiO	0.000	0.202	0.055	0.052		0.052	0.046	0.052	0.073	0.053	0.059	0.065	0.043
MnO	0.00	0.03	0.01	0.01		0.006	0.008	0.008	0.007	0.007	0.006	0.007	0.008
ZnO	0.000	0.070	0.008	0.011		0.005	0.005	0.011	0.010	0.010	0.006	0.012	0.004
MgO	0.00	0.51	0.09	0.07		0.086	0.104	0.074	0.087	0.121	0.064	0.092	0.090
CaO	0.000	0.187	0.018	0.024		0.007	0.006	0.012	0.024	0.022	0.022	0.018	0.043
Na_2O	0.000	0.000	0.000	0		0.000	0.000	0.000	0.000	0.000	0.000	0.000	0.000
K_2O	0.000	0.031	0.002	0.004		0.002	0.002	0.003	0.002	0.002	0.002	0.002	0.007
F	0.000	0.007	0.001	0.001		0.001	0.001	0.000	0.001	0.001	0.001	0.001	0.000
Cl	0.000	0.024	0.005	0.005		0.002	0.004	0.006	0.006	0.007	0.004	0.004	0.006
Total	**98.35**	**101.49**	**100.26**	**0.54**		**100.37**	**100.76**	**100.64**	**100.12**	**100.28**	**100.32**	**100.02**	**99.16**

4.5 Quantitative mineral liberation

The quantitative mineral liberation results show that there is a substantial increase in area grade mineral liberation for ilmenite with a decrease in fraction size, while a similar, but lesser, increase is seen for the magnetite in the Profile 2 – 603 sample. For ilmenite, liberated grains (particles with >80 % ilmenite) increase from 28 % in the coarsest +425 µm fraction, through 53 % in the +212 µm fraction and 72 % in the +104 µm fraction and to the 83 % maximum in the +54 µm fraction (**Figure 11**). The finest -53 µm fraction has slightly lower liberation at 80 % liberated ilmenite grains. The non-liberated classes of the coarsest two fractions consist mostly of composite and locked particles in a 2:1 ratio, while the three finest fractions consist mostly of composite particles and less than 5 % locked particles.

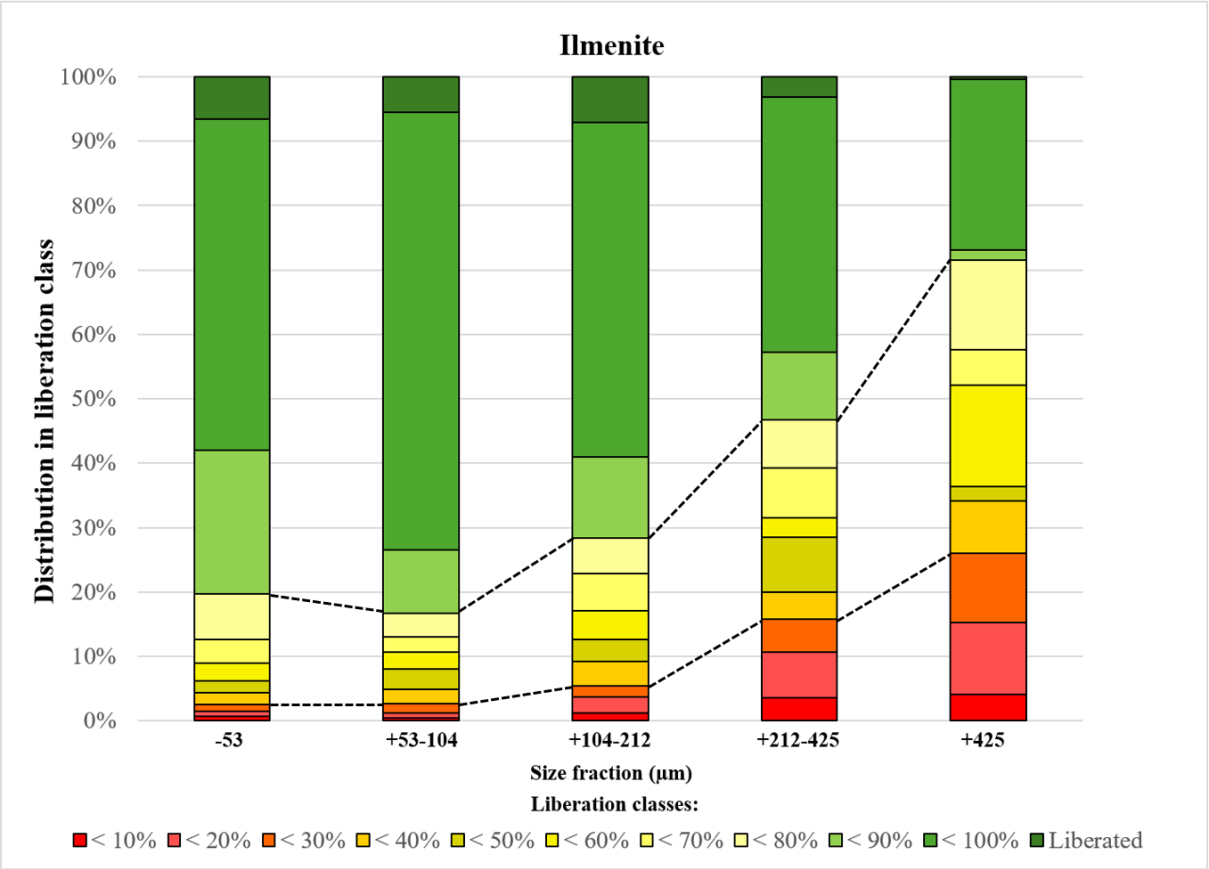

Figure 11: *Ilmenite area grade liberation data by fractions of Profile 2 – 603 of the Storgangen tailings. Distribution of grains in liberation classes. Locked = <10 % to <30 %, composite = <40 % to <80 %, liberated = <90 % to Liberated (100 %). Dotted lines display the trends between liberated (green), composite (yellow) and locked (red) classes.*

The magnetite shows a much lower liberation and a more gradual area grade liberation trend than the ilmenite (**Figure 12**). In the coarsest +425 µm fraction, only 22 % of the particles are liberated, while 50 % of the particles are in the locked classes. The +212 µm fraction shows a similar amount of liberated particles, but with 38 % locked particles. Liberation increases in the +104 µm fraction to 40% and peaks in the +53 µm fraction at 51% liberated particles, with 14% locked particles. Similar to ilmenite, magnetite shows decreased liberation in the finest fraction (-53 µm), at 38%.

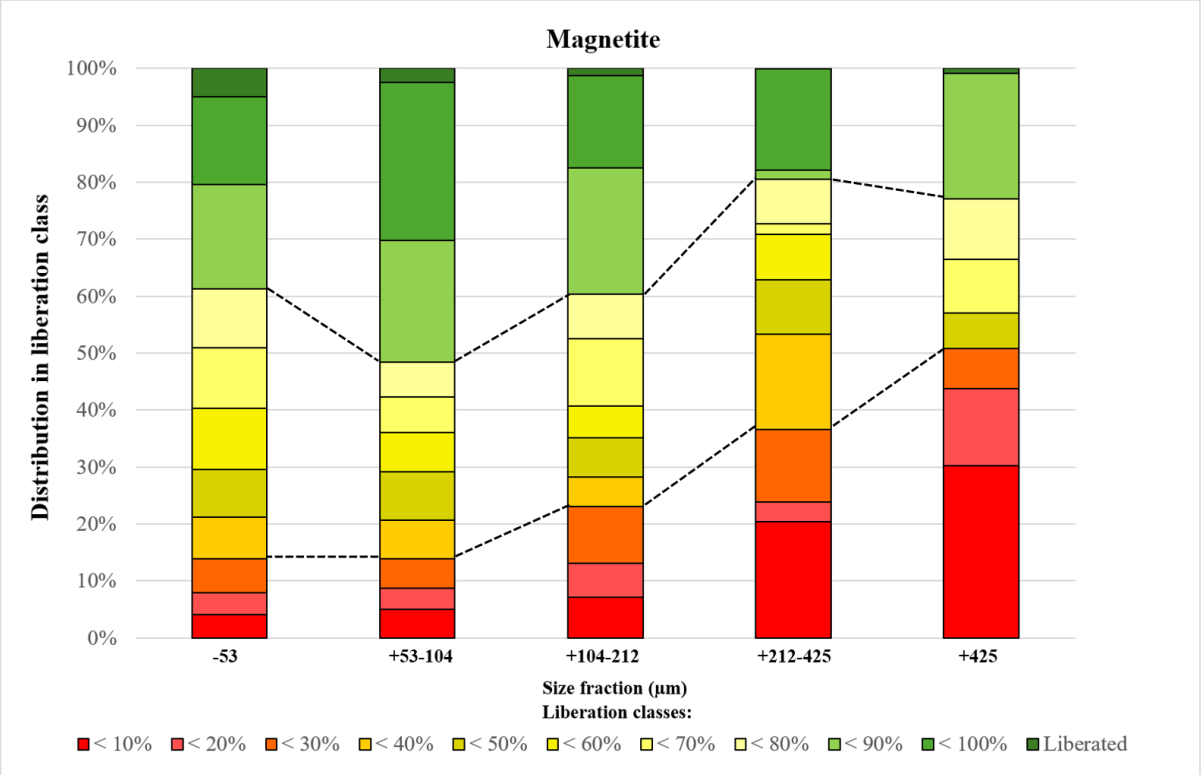

***Figure 12**: Magnetite area grade liberation data by fractions of Profile 2 – 603 of the Storgangen tailings. Distribution of grains in liberation classes. Locked = <10 % to <30 %, composite = <40 % to <80 %, liberated = <90 % to Liberated (100 %). Dotted lines display the trends between liberated (green), composite (yellow) and locked classes (red).*

4.6 Ilmenite and magnetite estimates

A very preliminary and rough estimate of the ilmenite and magnetite tonnages is calculated by the particle size distribution and weight per cent of ilmenite and magnetite by fraction of Profile 2 – 603, given a total tonnage of the tailings deposit of 6 million tonnes as reported in Nilsen (2015) (**Table 6**). Profile 2 – 603 has the highest TiO_2 and Fe_2O_3 content in the bulk chemistry assay. The estimate yields 850207 tonnes of ilmenite and 118 106 tonnes of magnetite. For ilmenite, the two finer fractions constitute a small portion of the total amount: 4.75% in the finest fraction (-53 µm), and 13.83 in the second finest fraction (+53 µm). Magnetite has a higher percentage in the two finest fractions compared to ilmenite, with 21.82% in the finest (-53 µm) and 12.26% in the second finest (+53 µm).

Table 6: *Initial estimate of ilmenite and magnetite content based on particle size distribution of Profile 2 – 603, and the weight per cent of ilmenite and magnetite by fraction of Profile 2 – 603, given a total tonnage of 6 Mt as reported in Nilsen (2015). C.Vol % = cumulative volume per cent, Wt. % = weight per cent.*

	-53 µm	**+53-104 µm**	**+104-212 µm**	**+212-425 µm**	**+425 µm**	**Total**
C. Vol %	2.4	8.48	25.42	36.46	27.24	100
Tonnage	144000	508800	1525200	2181600	1634400	**6000000**
Wt. % Ilmenite	28.04	23.11	11.22	9.30	19.48	-
Tonnage Ilmenite	40378	117558	171066	202823	318381	**850207**
Ilmenite (%)	4.75	13.83	20.12	23.86	37.45	100
Wt. % FeOx	17.89	2.85	1.41	1.26	1.78	-
Tonnage FeOx	25766	14475	21475	27379	29011	**118106**
Magnetite (%)	21.82	12.26	18.18	23.18	24.56	100

5. Discussion

This discussion is a rough draft based on SEM-AM results for one profile; post-processing is being finalised, and results for the remaining three will be added to the final paper. However, PSD, XRF and EPMA data are presented for all four profiles and show similar results.

5.1 The composition of the Storgangen tailings

The Storgangen tailings at the Sandbekk tailings storage facility are composed of over 80 Wt.% gangue minerals, mostly plagioclase and orthopyroxene, up to 14 Wt.% ilmenite and 2 Wt.% magnetite based on the highest grade samples presented in **Table 6**. This yields a maximum estimate of 850 000 tonnes of ilmenite and 118 000 tonnes of magnetite in the tailings, based on a total of 6 million tonnes of tailings at Sandbekk.

The particle size distribution of the samples analysed shows material that mostly consists of sand, with only 1.6 to 4% of the cumulative volume as coarse silt. Comparing the ilmenite and magnetite grade of the sieved fractions to the cumulative volume of each fraction yields the distribution of ilmenite and magnetite by size fraction. The majority of the ilmenite is found in the middle and top fractions: 37.45 % of the ilmenite is found in the top fraction (+425 µm), and 23.86% and 20.12% in the two middle fractions (+212 µm and +104 µm). In the two finest fractions, there is only 13.83 % (+53 µm) and 4.75 % (-53 µm). For magnetite, there is an enrichment from around 2 to 3 Wt.% in all fractions above +53 µm to 17.89 Wt.% in the finest fraction (-53

µm), resulting in an even distribution between the fractions. The magnetite of Profile 2 – 603 is roughly divided 50/50 between samples above and below 212 µm.

The tailings storage facility at Sandbekk is divided into three parts (**Figure 1**): Hauglandsmyr accounting for the earliest part of production from 1916 up until the mid-1930s; Kjerdal, which constitutes the majority of the tailings storage facility; and the tailings in the open pit of the Storgangen mine representing the final stages of tailings deposition at Sandbekk. No detailed spatial or characterising description of the deposited material exists. The implementation of flotation in processing at Sandbekk in the early 1950s likely increased ilmenite recovery and decreased ilmenite in the deposited tailings. The resolution of this study with four profiles is too low to say this for certain; however, initial investigations show that Profile 2 on Hauglandsmyr has the highest bulk TiO_2 content (5.49 %), while Profile 4 in the open pit of the Storgangen mine has the lowest (3.32 %). The bulk chemistry of all four profiles is fairly consistent, with TiO_2 ranging from 3.32 to 5.49 % and Fe_2O_3 from 9.89 to 15.61 %. The final paper will compare chemistry and automated mineralogy. For the first five years of production of the Storgangen mine, all magnetite was deposited with the tailings. This should be situated in the lower Hauglandsmyr area of the tailings storage facility, which is mostly revegetated.

5.2 Fe-Ti-V and Ni-Cu-Co deportment in the Storgangen tailings

The Fe-Ti-V deportment of the Storgangen tailings is mostly attributed to the ilmenite and magnetite. It will be commented on in the final paper once the Fe-Ti assay data and all SEM-AM data have been post-processed.

There is an enrichment of Ni and Co, and especially Cu in trace element analyses of the finest fractions (-53 µm) of the Storgangen tailings samples. This led to the expectation of finding more sulphides (pentlandite, millerite, siegenite, and chalcopyrite) in the SEM-AM scans of the finest fractions; however, mostly a few grains of pyrite were found. This suggests that little of the original Ni-Cu-Co phases survived the 110 to 61 years at Sandbekk, and that the high Ni, Cu, and Co contents must be present as altered products.

5.3 Potential for revalorisation of the Storgangen tailings

Given the initial mineralogical and liberation results, it could be possible to produce an ilmenite concentrate using state-of-the-art flotation cells on the tailings material between 20 and 212 µm (Wills & Finch, 2016). For magnetite, it could be possible to produce a concentrate with LIMS magnetic separation (Wills & Finch, 2016). A sieving stage should be implemented to separate the material finer than 212 µm from the coarser material. The

finer material can then be reprocessed simultaneously as the coarser material is reground to improve mineral liberation.

Regarding the potential for a Ni-Cu-Co concentrate, no related sulphide phases were observed in the finest fraction samples using SEM-Automated mineralogy, indicating their presence as alteration products. Leaching of these elements from water could be a processing route, but their current state needs to be determined first.

6. Conclusions

- Preliminary investigations of the Sandbekk tailings storage facility yield ilmenite contents of up to 14% in the tailings, with most ilmenite contained in fractions coarser than 53 µm.
- In the fractions finer than 425 µm, over 50% of the ilmenite is liberated, with the highest liberation found in the <212 µm fractions, where 72 to 83 % of the ilmenite is in liberated classes.
- It could be possible to produce an ilmenite concentrate on the tailings finer than 212 µm with state-of-the-art flotation cells.
- Magnetite constitutes only 2- 3 wt.% of the fractions coarser than 53 µm, but 17.89 Wt.% of the finest fraction (-53 µm).
- In the fractions coarser than 212 µm, around 20% of the magnetite is liberated, with the peak of liberation in the +53- 104 µm fraction, with 51% liberated particles, and 40% liberated particles in the -53 µm and +104-212 µm fractions.
- Production of a magnetite concentrate could be possible using LIMS magnetic separation on the tailings finer than 212 µm.
- Despite a significant enrichment of Ni-Cu-Co in the chemical analyses of the finest fractions, no associated Ni-Cu-Co minerals were observed in the polished sections, indicating that most of the Ni-Cu-Co minerals are altered and present as secondary alteration phases.

Declaration of competing interests

The authors declare that they have no known competing financial interests or personal relationships that could have appeared to influence the work reported in this paper.

Acknowledgements

This study is part of the first author's PhD thesis. The Research Council of Norway is acknowledged for the support to the Norwegian Laboratory for Mineral and Materials Characterisation, MiMaC, project number 269842/F50. The authors thank Torill Sørløkk, Jostein Røstad, Stefanie Lode, and Marek Zastapilo (NTNU) for their analytical assistance, and Titania AS for their cooperation and help with the sampling campaign and literature search. This project has received funding from the European Union in the framework of the Horizon Europe AVANTIS project under Grant Agreement No. 101137552.

Funded by the European Union

References

ALS. (2026, May 18). *Geochemistry Fee Schedule - 2026 Schedule of Services & Fees.* Retrieved from alsglobal.com: https://www.alsglobal.com/en/geochemistry/geochemistry-fee-schedules

Apeland, N. (1956). *På besøk ved Titania A.s.* Bergverks-Nytt nr. 9 p.11.

Ashwal, L., & Bybee, G. (2017). Crustal evolution and the temporality of anorthosites. *Earth-Science Reviews*, 307-330.

Bhuwalka, K., Field, III, F. R., De Kleine, R. D., Kim, H. C., Wallington, T. J., & Kirchain, R. E. (2021). Characterizing the Changes in Material Use due to Vehicle Electrification. *Sustainable Systems*, 10097-10107.

Blengini, G., Mancini, L., Mathieux, F., Nyberg, M., & Viegas, H. (2019). *Recovery of critical and other raw materials from mining waste and landfills - State of play on existing practices.* Publications Office of the European Union.

Bookhagen, B., Bastian, D., Buchholz, P., Faulstich, M., Opper, C., Irrgeher, J., . . . Koeberl, C. (2020). Metallic resources in smartphones. *Resources Policy*.

Bybee, G. M., Ashwal, L. D., Shirey, S., Horan, M., Mock, T., & Andersen, T. (2014). Pyroxene megacrysts in Proterozoic anorthosites: Implications for tectonic setting, magma source and magmatic processes at the Moho. *Earth and Planetary Science Letters, 389*, 74-85.

Calvo, G., Mudd, G., Valero, A., & Valero, A. (2016). Decreasing Ore Grades in Global Metallic Mining: A Theoretical Issue or A Global Reality? *Resources*.

Carstens, H. (2002). *Titania i 100! Jubileumsbok for Titania A/S.* Hauge i Dalane: Titania A/S.

Duchesne, J., & Bingen, B. (2001). The Rogaland Anorthosite Province: An Introduction. In J. Duchesne, *The Rogaland Intrusive Massifs - an excursion guide* (pp. 139; 13-22). Trondheim: Geological Survey of Norway.

Duchesne, J.-C. (1999). Fe-Ti deposits in Rogaland anorthosites (South Norway): geochemical characteristics and problems of interpretation. *Mineralium Deposita, 34*, 182-198.

European Commission. (2020). COM (2020) 474 - Critical Raw Materials Resilience: Charting a Path towards greater Security and Sustainability.

European Commission. (2024, August 22). *Critical Raw Materials Act*. Retrieved from single-market-economy.ec.europa.eu: https://single-market-economy.ec.europa.eu/sectors/raw-materials/areas-specific-interest/critical-raw-materials/critical-raw-materials-act_en

Habashi, F. (2013). The Seven Metals of Antiquity. *Mineral Processing and Extractive Metallurgy IMM Transactions section C*, 190-191.

Krause, H., & Pape, H. (1975). Mikroskopische Untersuchungen Der Mineralvergasellschaftung in Erz und Nebengstein der Ilmenitlagetstätte Storgangen (Süd-Norwegen). *Norsk Geologisk Tidsskrift*, 387-422.

Kullerud, K. (2003). *Geochemistry and mineralogy of the Tellnes ore body.* Hauge i dalane: Titania AS.

Kullerud, K. (2007). *Compositional variations of the Tellnes ore in the Skogestad area.* Hauge i dalane: Titania AS.

Magrini, C., Verga, F., Bassani, I., Pirri, C. F., & Azim, A. A. (2025). A Microbial-Centric View of Mobile Phones: Enhancing the Technological Feasability of Biotechnological Recovery of Critical Metals. *Bioengineering*.

Mansur, E., Orvik, A. A., Coint, N., Huyskens, M. H., Slagstad, T., Schiellerup, H., & Dare, S. (2025). Formation of Fe-Ti Deposit Within an Open-System Magmatic Chamber: Insights from the Storgangen Deposit, Rogaland Anorthosite Province, Southwest Norway. *Economic Geology*, 1555-1575.

Marker, M., Bolle, O., Robins, B., Meyer, G., & Schiellerup, H. (2004). *Geological map of the Rogaland Anorthosite Province - Scale 1 : 75 000 NGU Report 2004.007.* Trondheim: NGU.

Namur, O., Hatert, F., Grandjean, F., Long, G. J., Krins, N., Fransolet, A.-M., . . . Charlier, B. (2009). Ti substitution mechanisms in phlogopites from the Suwalki massif-type anorthosite, NE Poland. *European Journal of Mineralogy*, 397-406.

Nilsen, A. H. (2015). *100 år med deponering.* Titania AS.

Oberle, B., Brereton, D., & Mihaylova, A. (2020). *Towards zero harm: A compendium of papers prepared for the Global Tailings Review.* London: Global Tailings Review.

Osen, J. (2024). *A preliminary study of the Ni-Cu-Co sulphide concentrator at Titania AS.* Trondheim: Norwegian University of Science and Technology.

Røisi, I. (2018). *Standard operational procedure IGP: Preparation of regular polished sections and vertically cut polished sections of mineral particulates for automated mineralogy.* Trondheim: NTNU, IGP.

Røisi, I., & Aasly, K. (2018). The effect of graphite filler in sample preparation for automated mineralogy - a preliminary study. *Mineralproduksjon 8*, A1-A23.

Schärer, U., Wilmart, E., & Duchesne, J. (1996). The short duration and anorogenic character of anorthosite magmatism: U-Pb dating of the Rogaland complex, Norway. . *Earth and Planetary Science Letters 139*, 335-350.

Schiellerup, H. (1996). *Fe-Ti mines and prospects in the Egersund area of the South Rogaland Igneous Province. Field report, 1995.* Trondheim: NGU.

Slagstad, T., Henderson, I. H., Roberts, N. M., Kulakov, E. V., Ganerød, M., Kirkland, C. L., . . . Coint, N. (2022). Anorthosite formation and emplacement coupled with differential tectonic exhumation of

ultrahigh-temperature rocks in a Sveconorwegian continental back-arc setting. *Precambrian research, 376*.

Slagstad, T., Roberts, N. M., Marker, M., Røhr, T. S., & Schiellerup, H. (2013). A non-collisional, accretionary Sveconorwegian orogen. *Terra Nova, 25*, 20-37.

Titania A/S. (1992). *Ilmenitten - Titania A/S 90 år 1902 - 1992.* (K. Immerstein, Ed.) Titania A/S.

United Nations Environment Programme, International Council on Mining and Metals, Principles for Responsible Investment. (2020). *Global Industry Standard on Tailings Management.* United Nations Environment Programme. Retrieved from https://wedocs.unep.org/handle/20.500.11822/36139

van Gerve, T. D., Muchez, P., Nuorivaara, T., & Namur, O. (2026). The impact of exsolution textures in Fe-Ti oxide minerals on crushing strategies and vanadium and titanium pre-concentration. *European Journal of Mineralogy, 38*, 545-556.

Warr, L. N. (2021). IMA-CNMNC approved mineral symbols. *Mineralogical Magazine*, 291-320.

Wentworth, C. K. (1922). A Scale of Grade and Class Terms for Clastic Sediments. *The Journal of Geology, 30*, 377-392.

Wills, B. A., & Finch, J. A. (2016). *Wills´s Mineral Processing Technology An introduction to the Practical Aspects of Ore Treatment and Mineral Recovery* (Eighth Edition ed.). Butterworth-Heinemann.

Wilson, J., Robins, B., Nielsen, F., Duchesne, J., & Vander Auwera, J. (1996). The Bjerkreim-Sokndal Layered Intrusion, Southwest Norway. *Developments in Petrology*, 231-255.